Food Control 36 (2014) 49–54

Contents lists available at ScienceDirect

Food Control

journal homepage: www.elsevier.com/locate/foodcont

Development of acetylcholinesterase biosensor based on platinum–carbon aerogels composite for determination of organophosphorus pesticides

Yong Liu [a], Min Wei [b,*]

[a] Institute of Fine Chemistry and Engineering, College of Chemistry and Chemical Engineering, Henan University, Kaifeng 475004, PR China
[b] College of Food Science and Technology, Henan University of Technology, Zhengzhou 450052, PR China

ARTICLE INFO

Article history:
Received 20 February 2013
Received in revised form
2 August 2013
Accepted 6 August 2013

Keywords:
AChE biosensor
Pt–CAs composite
Methamidophos
Monocrotophos

ABSTRACT

A fast, sensitive and stable acetylcholinesterase (AChE) biosensor was developed based on platinum–carbon aerogels (Pt–CAs) composite to detect organophosphorous pesticides (OPs). The Pt–CAs composite was prepared by the sol–gel polymerization and the ethylene glycol liquid-phase reduction method, then was firstly used to modify boron-doped diamond (BDD) electrode for AChE immobilization. The electron transfer resistance of the Pt–CAs/BDD electrode was smaller than that of the bare BDD electrode, indicating that the presence of Pt–CAs composite on the electrode surface could improve the reactive site, reduce the interfacial resistance, and make the electron transfer easier. In comparison with AChE/BDD electrode, the negative shift of peak potential and the increase of peak current upon the oxidation of thiocholine were obtained on AChE/Pt–CAs/BDD electrode. Using methamidophos as model compound, the conditions for OPs detection were optimized. Under the optimized conditions, the inhibition rate of methamidophos and monocrotophos were linearly proportional to their concentrations in the range of 10^{-11}–10^{-6} M. The detection limits were found to be 3.1×10^{-13} M (0.05 ppt) for methamidophos and 2.7×10^{-12} M (0.6 ppt) for monocrotophos. The developed biosensor exhibited good reproducibility and acceptable stability.

1. Introduction

Organophosphorus pesticides (OPs) play an important role in controlling insects in agricultural fields. However, overuse of OPs results in pesticide residues in food, water and environment, causing a severe threat to human health because OPs can inhibit the activity of acetylcholinesterase (AChE), which regulates acetylcholine, a neurotransmitter needed for proper nervous system function. Inhibiting AChE activity makes acetylcholine disorder, leading to fatal consequences such as respiratory paralysis and death (Guo, Zhan, Cai, Shen, & Zhu, 2013; Liu et al., 2012; Wei et al., 2012). Therefore, for the sake of food safety and environment protection, it is of great importance to find ways to rapidly determinate the trace level of OPs. To obtain this aim, different detection technologies were developed (Ballesteros & Parrado, 2004; Gao, Tang, & Su, 2012; Sun, Zhu, & Wang, 2012; Uutela, Reinila, Piepponen, Ketola, & Kostiainen, 2005). Among them, electrochemical biosensors based on the inhibition of AChE are regarded as highly promising candidates for OPs detection (Du, Chen, Cai, & Zhang, 2007; Zejli et al., 2008) because of their advantages with rapidity, simplicity and economy. This method employs enzymatic activity as an indicator for quantitative measurement of OPs. When AChE was immobilized on the working electrode surface, it catalyzes hydrolysis of acetylthiocholine (ATCl), and the resultant product is electro-active thiocholine, which can produce an irreversible oxidation peak. The oxidation current of thiocholine is inversely proportional to the concentration of OPs.

To fabricate AChE biosensor, immobilizing AChE on the electrode surface is a crucial step. Different carbon materials such as exfoliated graphitic nanoplatelets (Ion et al., 2010), different functionalized grapheme (Li & Han, 2012; Wang et al., 2011; Zhang, Long, Zhang, Du, & Lin, 2012; Zhang, Zhang, Du, & Lin, 2012), mesoporous carbons and carbon black (Lee et al., 2010), carbon nanotube (Chauhan & Pundir, 2011; Kandimalla & Ju, 2006; Sharma et al., 2012; Zamfir, Rotariu, & Bala, 2011) have been successfully used to immobilize AChE due to their electrical conductivity, stability, and capacity to immobilize enzymes. Recently, carbon aerogels (CAs), as an alternative to the above-mentioned carbon

* Corresponding author.
E-mail address: wei_min80@163.com (M. Wei).

0956-7135/$ – see front matter © 2013 Elsevier Ltd. All rights reserved.
http://dx.doi.org/10.1016/j.foodcont.2013.08.005

materials, have attracted tremendous attention because of their many excellent properties such as high electrical conductivity, great mesopore volume and high accessible surface area. Thanks to these potentials, the CAs have been used as supports of precious metal for electrocatalytic reaction (Kim, Kim, Park, Park, & Suh, 2008; Machadoa et al., 2012; Maldonado-Hodar, 2012), whereas have seldom been used for immobilization of AChE. On the other hand, platinum nanoparticles (Pt) have also been reported to provide immobilization sites for the enzymes due to their excellent conductive property and compatibility (Bahshi, Frasconi, Tel-Vered, Yehezkeli, & Willner, 2008; Zhou et al., 2012).

In this work, Pt–CAs composite were prepared and firstly used to immobilize AChE. This composite is expected to retain the porous structure and inherit the advantages from its parent materials, thus provide a native environment to increase the enzyme loading. Using boron-doped diamond (BDD), a novel electrode material, as working electrode (Wei et al., 2008; Wei, Xie, Sun, & Gu, 2009), AChE/Pt–CAs/BDD biosensor were fabricated by directly immobilizing AChE on Pt–CAs modified BDD electrode, and their electrochemical behaviors were subsequently investigated by electrochemical impedance spectroscopy (EIS) and differential pulse voltammetry (DPV). Using methamidophos as model compound, the conditions for detection of OPs were optimized. The performance of proposed AChE/Pt–CAs/BDD biosensor was investigated in detail.

2. Experimental

2.1. Materials

Acetylcholinesterase (Type C3389, 500 U/mg from electric eel), acetylthiocholine chloride (ATCl) and bovine serum albumin (BSA) were purchased from Sigma–Aldrich (St. Louis, USA) and used as received. Methamidophos and Monocrotophos (≥99%) were obtained from Augsburg (Germany). 0.1 M phosphate buffer solution (PBS) was prepared by mixing stock solutions of NaH_2PO_4 and Na_2HPO_4 and adjusting the pH with 0.1 M HCl or 0.1 M NaOH. All other chemicals were of analytical-reagent grade and used without further purification. Double distilled water (DW) was used throughout the experiments.

2.2. Apparatus

All the electrochemical experiments were performed on a CHI 660D Electrochemical Workstation (Shanghai Chenhua Instrument Corporation, China). A three-electrode system was comprised of platinum wire as auxiliary electrode, Ag/AgCl as reference electrode and the modified or unmodified BDD as working electrode.

N_2 adsorption and desorption isotherms of CAs were measured at 77 K with Accelerated Surface Area and Porosimetry System (ASAP 2020, Micromeritics Instrument Corporation, USA). The specific surface areas of CAs were calculated with the Brunauer-Emmett-Teller (BET) method. The pore size distributions were calculated with the Barrerr-Joyner-Halenda (BJH) method.

Transmission electron microscopy (TEM) measurements were performed at 200 kV using JEM-2100UHR (JEOL Ltd., Japan).

2.3. Preparation of the Pt–CAs composite

CAs were synthesized by the sol–gel polymerization of resorcinol (R) and formaldehyde (F) in an aqueous solution according to the method described elsewhere (Babic, Kaluderovic, Vracar, & Krstajic, 2004). RF solution was prepared by mixing resorcinol, formaldehyde (37%), and deionized water (W), with sodium carbonate (C) as a basic catalyst. In this case, the R/F molar ratio was 0.5, the R/C molar ratio was 300, and the R/W molar ratio was 0.05. The homogeneous RF solution was put into glass tube, and was subsequently sealed. The tube was respectively kept at room temperature, 50 °C and 85 °C for 24 h. The hydrogels were exchanged with acetone three times to remove water. The samples were dried with conventional CO_2 supercritical drying method (Horikawa, Hayashi, & Muroyama, 2004). Organic RF aerogels were carbonized in a horizontal vacuum tubular furnace under nitrogen flow. The samples were heated up to 900 °C at 5 °C min^{-1}, and the final temperature was kept for 3 h. At last, the furnace was cooled to room temperature.

The Pt–CAs composite were synthesized by the ethylene glycol (EG) liquid-phase reduction method (Wei, Wu, Shang, & Fu, 2009). CAs (80 mg) were mixed with 150 ml of EG under ultrasonic treatment for 30 min to form a homogeneous slurry. The solution of H_2PtCl_6 in EG containing 20 mg of Pt was slowly added into the CAs slurry. The mixture was stirred for 2 h for impregnation. Then the pH value of the mixture slurry was adjusted to 10 by using 0.5 M NaOH solution in EG solution. The slurry was heated to 130 °C and maintained for 3 h. The mixture was filtered and washed thoroughly by deionized water after cooling, then dried at 50 °C for 12 h in air, finally, the Pt–CAs composite were obtained.

2.4. Fabrication of AChE biosensor

BDD electrode was ultrasonicated successively in anhydrous ethanol, acetone and DW, and then was dried at room temperature before use. The AChE/Pt–CAs/BDD biosensor was prepared as follows: Firstly, 5 mg Pt–CAs composite was ultrasonically dispersed in 10 ml mixture solution of isopro-propanol and DW for 30 min to form a homogeneous ink. The BDD electrode was spread with 10 μL Pt–CAs composite solution, and dried at room temperature. Then 10.0 μL AChE solution (containing 1% BSA to maintain the stability of AChE) was dropped on Pt–CAs/BDD electrode and incubated at 25 °C for 30 min. After water was evaporated, the modified electrode was washed with PBS (0.1 M, pH 7.3) to remove the unbound AChE, and the obtained AChE/Pt–CAs/BDD biosensor was stored at 4 °C when not in use.

2.5. Measurement procedure

To measure methamidophos and monocrotophos, the obtained AChE/Pt–CAs/BDD was first immersed in PBS (pH 7.3) solution containing 1.0 mM ATCl as substrate. After that, different concentration of standard methamidophos and monocrotophos were added into the electrochemical cell to investigate the electrochemical response by differential pulse voltammetry (DPV). The inhibition rate of pesticides was determined according to the expression (Stoytcheva et al., 2009), and the inhibition of methamidophos and monocrotophos is calculated as follows: inhibition $(\%) = [(I_0 - I)/I_0] \times 100\%$. where I_0 is the peak current of thiocholine, hydrolysis product of ATCl on the AChE/Pt–CAs/BDD and I is that with methamidophos and monocrotophos inhibition.

2.6. Analysis of methamidophos and monocrotophos in spiked apple juice samples

The apple juice was purchased from a local supermarket in China. The pH of juices was adjusted to ~7.3 by 0.1 M NaOH. Several methamidophos and monocrotophos standard solutions were mixed into the apple juice samples to obtain final concentrations of 0.1, 1, and 10 nM. The apple juice samples were filtered through a 0.22 μm filter (Guo et al., 2013), and the filtrates were tested using the as-prepared AChE/Pt–CAs/BDD biosensor.

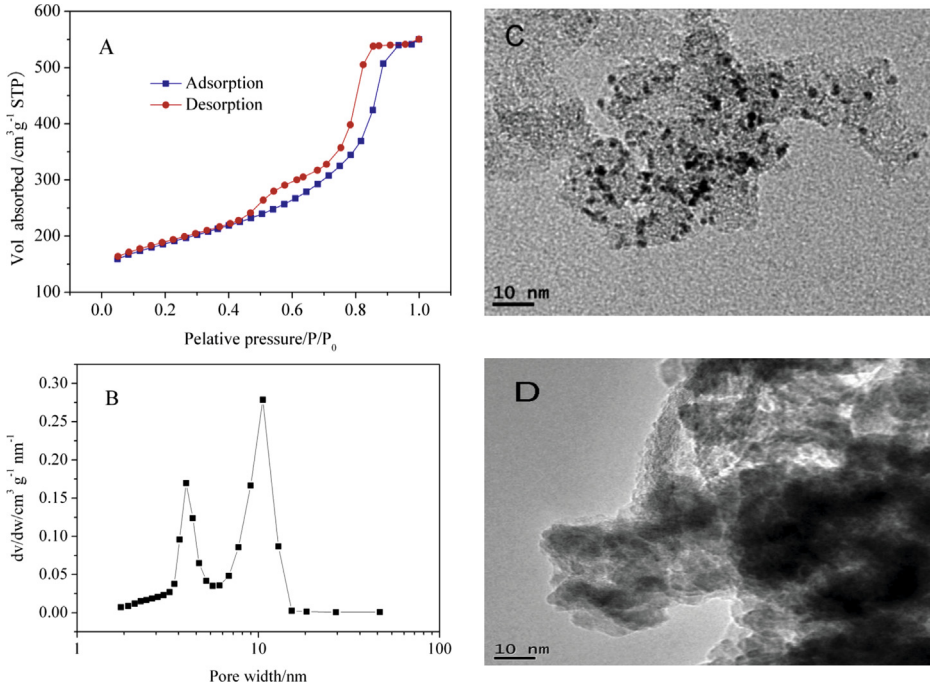

Fig. 1. (A) The N_2 adsorption and desorption isotherms and (B) pore size distributions of CAs. (C) TEM image of Pt–CAs composite. (D) TEM image of AChE/Pt–CAs.

3. Results and discussion

3.1. Characterization of prepared materials

The surface area and textural characteristics of the prepared CAs were characterized by using N_2 adsorption and desorption isotherms, and the results were shown in Fig. 1A. The CAs samples showed a type IV according to IUPAC classification (Sing et al., 1985), which indicated that mesopores has existed in the samples. The pore size distribution of CAs calculated by the BJH method according to N_2 adsorption isotherm was shown in Fig. 1B. The CAs has mesoporous structure with average pore size of 9.8 nm. BET surface area of CAs is 616 $m^2\,g^{-1}$, which is far larger than the surface area of commercial Vulcan XC-72R (254 $m^2\,g^{-1}$). Fig. 1C presented the TEM image of Pt–CAs composite. It can be seen that little agglomeration of particles was observed on the CAs supports, indicating that the Pt nanoparticles were adhered to the surface of the CAs. Fig. 1D showed the TEM image of AChE/Pt–CAs. The enhancement of opacity and obscurity demonstrated the AChE has been successfully immobilized.

3.2. Electrochemical behaviors of the AChE/Pt–CAs/BDD biosensor

Electrochemical impedance spectroscopy (EIS) was used to characterize the preparation process of AChE/Pt–CAs/BDD biosensor. As shown in Fig. 2, the electron transfer resistance (Rct) of the Pt–CAs/BDD electrode (~360 Ω, Fig. 2b) was smaller than that of the bare BDD electrode (~590 Ω, Fig. 2a), which indicated that the presence of Pt–CAs composite on the electrode surface improved the reactive site, reduced the interfacial resistance, and made the electron transfer easier, which can be ascribed to their great mesopore volume, high accessible surface, and excellent conductive property. The remarkable increase of Rct on the AChE/Pt–CAs/BDD electrode (~850 Ω, Fig. 2c) confirmed the successful immobilization of AChE.

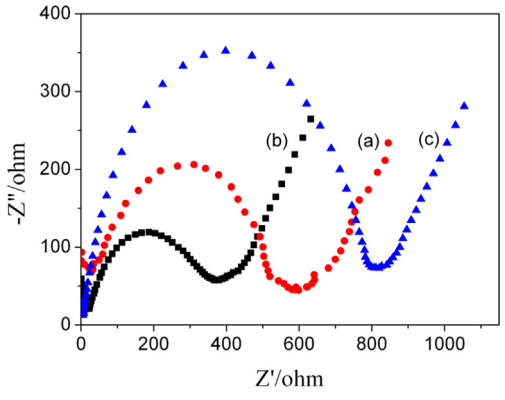

Fig. 2. Nyquist plot of EIS in 0.1 M KCl solution containing 1×10^{-2} M $[Fe(CN)_6]^{3-/4-}$ at (a) bare BDD electrode, (b) Pt–CAs/BDD electrode, and (c) AChE/Pt–CAs/BDD electrode. Frequency range: 0.1 Hz to 10 kHz.

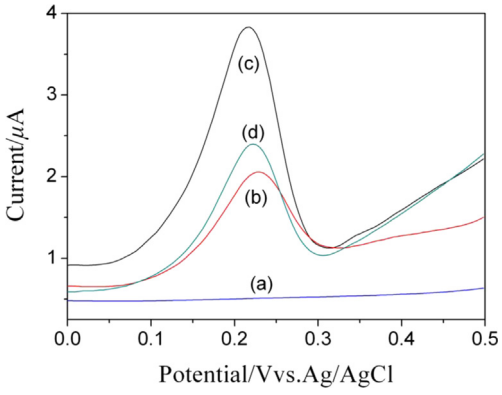

Fig. 3. DPV response of different electrode in pH 7.3 PBS containing 1.0 mM ATCl. (a) bare BDD electrode, (b) AChE/BDD electrode, and (c) AChE/Pt–CAs/BDD electrode. (d) DPV response of AChE/Pt–CAs/BDD electrode after inhibition in 10 nM methamidophos solution for 10 min.

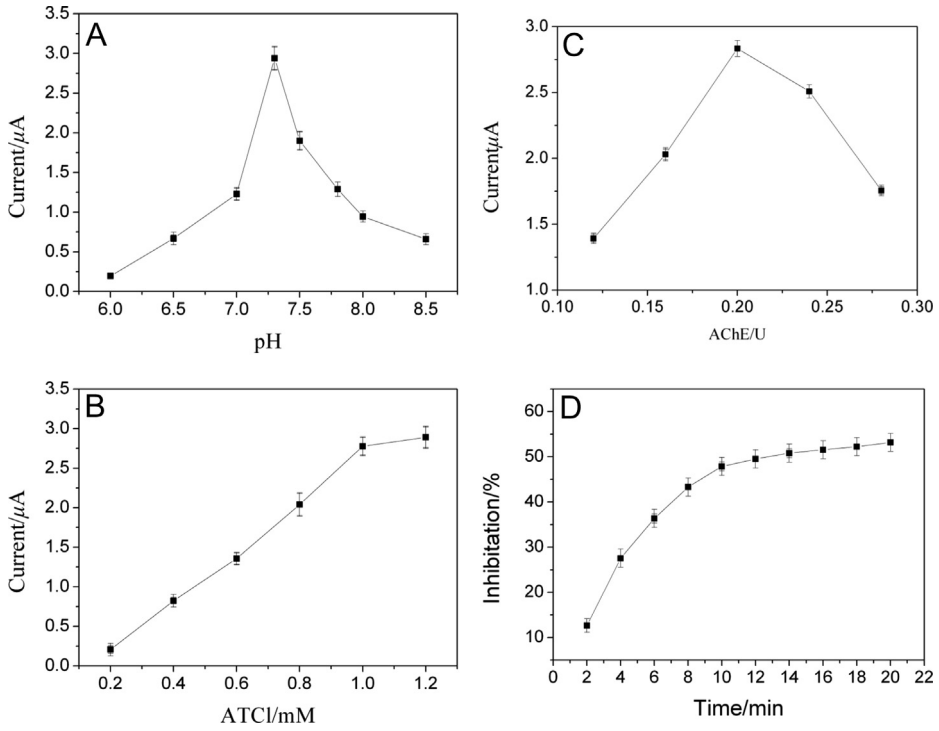

Fig. 4. Effects of pH (A), ATCl concentration (B), AChE loading (C) and inhibition time (D) on the response of AChE/Pt–CAs/BDD biosensor.

DPV response on different electrodes was studied in pH 7.3 PBS containing 1.0 mM ATCl, and the results are shown in Fig. 3. No detectable signal was observed on the bare BDD electrode (Fig. 3a), whereas obvious oxidation peaks were showed on AChE/BDD electrode (Fig. 3b) and AChE/Pt–CAs/BDD electrode (Fig. 3c). Obviously, these peaks came from the oxidation of thiocholine, hydrolysis product of ATCl, catalyzed by the immobilized AChE. The oxidation peak current of thiocholine was 1.160 μA at ~0.230 V on the AChE/BDD electrode (Fig. 3b), and got to 2.770 μA at ~0.218 V on the AChE/Pt–CAs/BDD electrode (Fig. 3c).The peak potential was negatively shifted by 0.022 v, and the peak current was increased by 138.79%, which can be ascribed to that the Pt–CAs composite could increase the surface area, promote AChE adsorption, enhance the activity of AChE, promote the electrocatalytic ability, and accelerate the electron transfer (Bahshi et al., 2008; Kim et al., 2008).

Fig. 3d showed DPV response of AChE/Pt–CAs/BDD electrode after inhibition in 10 nM methamidophos solution for 10 min. In comparison with that for 0 min (Fig. 3c), when AChE/Pt–CAs/BDD was immersed in 10 nM methamidophos solution for 10 min, the oxidation peak current of thiocholine decreased from 2.770 μA to 1.490 μA, and the inhibition rate was 46.21%. This was because that methamidophos, as one of the OPs, exhibited high toxicity and involved in the irreversible inhibition action on AChE activity, thus reducing the product of thiocholine (Gong, Guan, & Song, 2013; Jha & Ramaprabhu, 2010). According to the obvious change in electrochemical signal on the AChE/Pt–CAs/BDD electrode, the simple and rapid method for determination of methamidophos could be established.

3.3. Optimization of parameters

The effect of solution pH on the peak current response was studied in series of PBS containing 1.0 mM ATCl with the pH from 6.0 to 8.5 by DPV. As shown in Fig. 4A, the maximum response peak current appeared at pH 7.3. Thus pH 7.3 was selected subsequent experiments.

The effect of ATCl concentration on the biosensor response from 0.2 to 1.2 mM was investigated and the results were shown in

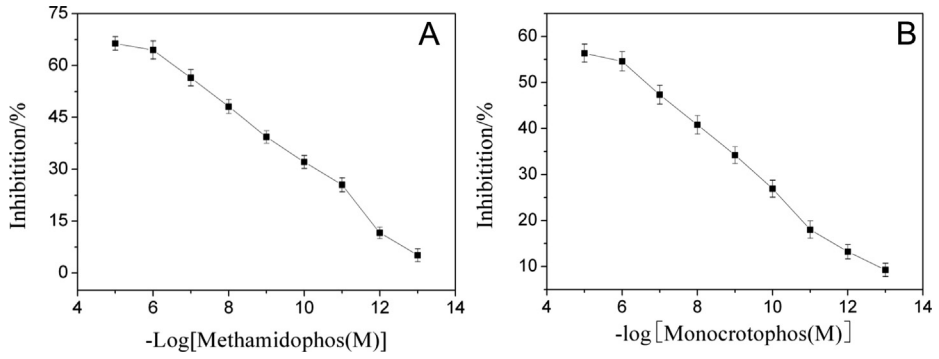

Fig. 5. The inhibition of the AChE/Pt–CAs/BDD biosensor versus the logarithm of methamidophos concentration (A) and monocrotophos concentration (B).

Table 1
Comparison with other reported biosensors for methamidophos and monocrotophos detection.

Electrode material	Linearity	Detection limit	Analyte	References
AuNPs-MWCNTs-CM	0.1–10 μM	10 nM (1×10^{-8} M)	Monocrotophos	Norouzi, Pirali-Hamedani, Ganjali, & Faridbod, 2010
AuNPs–SiSG	0.001–1 ppm	0.6 ppb (2.69×10^{-9} M)	Monocrotophos	Du et al., 2007
CdTe-AuNPs-CM	1–1000 ppb	0.3 ppb (1.34×10^{-9} M)	Monocrotophos	Du, Chen, Song, Li, & Chen, 2008
MSF-PVA	0.05–10 ppb	0.05 ppb (2×10^{-10} M)	Monocrotophos	Wu et al., 2011
Pt-Cas	10^{-11}–10^{-6} M	2.7×10^{-12} M	Monocrotophos	This work
AuNPs	28×10^{-3}–170×10^{-3} μM	7.0×10^{-3} μM (7×10^{-9} M)	Methamidophos	Li et al., 2010
TCNQ	0.5–100 ppb	1 ppb (4×10^{-9} M)	Methamidophos	Marques, Nunes, dos Santos, Andreescu, & Marty, 2004
Pt-Cas	10^{-11}–10^{-6} M	3.1×10^{-13} M	Methamidophos	This work

Fig. 4B. The response peak current increased obviously when ATCl concentration increased from 0.2 to 1.0 mM. However, there was no significant current improvement when the concentration increased to 1.2 mM, which revealed that the electrode had reached its saturation level. So, 1.0 mM ATCl was selected as optimum concentration for further experiments.

Fig. 4C displays the effect of AChE loading on biosensor response. The DPV peak current increased with increasing the amount of AChE and reached the maximum at 0.2 U, then decreased when the amount of AChE was increased further. This may be due to that the excess AChE could enhance the electrode resistance and slow the electron transfer between substrate and electrode. So, 0.2 U AChE was chosen as the optimal enzyme concentration.

The effect of inhibition time on biosensor response was also investigated. The AChE/Pt–CAs/BDD biosensor was incubated in a constant concentration of 10 nM methamidophos standard solution for different period of time. As shown in Fig. 4D, the inhibition showed obvious increase with the increase of inhibition time within 10 min however, when the inhibition time is longer than 10 min, there was no obvious increase, indicating an equilibration state. As a result, the optimum inhibition time was set at 10 min for the incubation steps in this study.

3.4. Calibration curve for methamidophos and monocrotophos detection

Based on the optimal experimental conditions, the relationship between inhibition rate of the AChE/Pt–CAs/BDD biosensor and different concentrations of methamidophos and monocrotophos was studied and the results were shown in Fig. 5. It was found that the relative inhibition increased when methamidophos concentrations and monocrotophos concentrations increased ranging from 10^{-13} to 10^{-5} M. For methamidophos, the linear equation was $y = 107.437 - 7.393x$ ($R^2 = 0.993$) within the linear range of 10^{-11}–10^{-6} M and the detection limit was 3.1×10^{-13} M (0.05 ppt) (calculated for 15% inhibition rate). For monocrotophos, the linear equation was $y = 97.875 - 7.164x$ ($R^2 = 0.997$) within the linear range of 10^{-11}–10^{-6} M and the detection limit was 2.7×10^{-12} M (0.6 ppt) (calculated for 15% inhibition rate) (Rotariu, Zamfir, & Bala, 2012; Zhao, Ge, Xu, & Chen, 2009). The comparison between the performance of the AChE/Pt–CAs/BDD biosensor in this study with other reported AChE biosensors was summarized in Table 1. It can be seen that compared with other methods, the present biosensor exhibited lower detection limit due to the fact that Pt–CAs composite could increase the surface area, raise AChE adsorption, enhance the activity of AChE, and promote electron transfer reactions.

Table 2
Recovery of methamidophos and monocrotophos in spiked apple juice samples ($n = 3$).

Pesticide	Added (nM)	Found (nM)	Recovery (%)	RSD (%)
Methamidophos	0.1	0.095	95	4.5
	1	0.989	98.9	5.7
	10	10.6	106	4.3
Monocrotophos	0.1	0.091	91	6.2
	1	0.971	97.1	4.3
	10	9.93	99.3	5.0

3.5. Reproducibility, stability of the AChE/Pt–CAs/BDD biosensor

The reproducibility of the AChE/Pt–CAs/BDD biosensor was evaluated by analyzing methamidophos levels for eight replicate measurements in 1.0 mM ATCl after being treated with 10 nM methamidophos for 10 min. Similarly, the inter-assay precision was estimated at five different electrodes for the determinations. The coefficient of variation of intra-assay and inter-assay was 3.48% and 4.63%, respectively, which indicated that the AChE/Pt–CAs/BDD biosensor was reproducible and precise. The prepared AChE/Pt–CAs/BDD biosensor was stored at 4 °C when not in use. After a 30-day storage period, the biosensor retained 94.49% of its initial current response, proving the acceptable stability.

3.6. Analysis of methamidophos and monocrotophos in spiked apple juice samples

Apple juices were spiked with varying concentration of methamidophos and monocrotophos as described in experimental section, and were measured to evaluate the reliability of the proposed AChE/Pt–CAs/BDD biosensor. As shown in Table 2, for methamidophos detection, the recoveries were found to be between 95% and 106%. For monocrotophos detection, the recoveries were found to be between 91% and 99.3%. The results indicated that the proposed biosensor is acceptably accurate and precise, and can be used for the analysis of samples from a real environment.

4. Conclusion

The Pt–CAs composite was successfully prepared and firstly used to develop a novel AChE biosensor for the detection of OPs. Owing to the excellent property of Pt–CAs composite such as high electrical conductivity, great mesopore volume, high accessible surface area, and good biocompatibility, the prepared AChE/Pt–CAs/BDD biosensor exhibited higher sensitivity, lower detection limit, good reproducibility and acceptable stability toward OPs detection.

Acknowledgments

This research was supported by National Natural Science Foundation of China (Grant No. 21105022), Doctor Foundation of Henan

University of Technology (2010BS019), and Plan for Scientific Innovation Talent of Henan University of Technology (2012CXRC01).

References

Babic, B., Kaluderovic, B., Vracar, L., & Krstajic, N. (2004). Characterization of carbon cryogel synthesized by sol–gel polycondensation and freeze-drying. *Carbon, 42*, 2617–2624.

Bahshi, L., Frasconi, M., Tel-Vered, R., Yehezkeli, O., & Willner, I. (2008). Following the biocatalytic activities of glucose oxidase by electrochemically cross-linked enzyme-Pt nanoparticles composite electrodes. *Analytical Chemistry, 80*, 8253–8259.

Ballesteros, E., & Parrado, M. J. (2004). Continuous solid-phase extraction and gas chromatographic determination of organophosphorus pesticides in natural and drinking waters. *Journal of Chromatography A, 1029*, 267–273.

Chauhan, N., & Pundir, C. S. (2011). An amperometric biosensor based on acetylcholinesterase immobilized onto iron oxide nanoparticles/multi-walled carbon nanotubes modified gold electrode for measurement of organophosphorus insecticides. *Analytica Chimica Acta, 701*, 66–74.

Du, D., Chen, S. Z., Cai, J., & Zhang, A. D. (2007). Immobilization of acetylcholinesterase on gold nanoparticles embedded in sol–gel film for amperometric detection of organophosphorous insecticide. *Biosensors and Bioelectronics, 23*, 130–134.

Du, D., Chen, S. Z., Song, D. D., Li, H. B., & Chen, X. (2008). Development of acetylcholinesterase biosensor based on CdTe quantum dots/gold nanoparticles modified chitosan microspheres interface. *Biosensors and Bioelectronics, 24*, 475–479.

Gao, X., Tang, G. C., & Su, X. G. (2012). Optical detection of organophosphorus compounds based on Mn-doped ZnSe d-dot enzymatic catalytic sensor. *Biosensors and Bioelectronics, 36*, 75–80.

Gong, J. M., Guan, Z. Q., & Song, D. D. (2013). Biosensor based on acetylcholinesterase immobilized onto layered double hydroxides for flow injection/amperometric detection of organophosphate pesticides. *Biosensors and Bioelectronics, 39*, 320–323.

Guo, X. S., Zhang, X. Y., Cai, Q., Shen, T., & Zhu, S. M. (2013). Developing a novel sensitive visual screening card for rapid detection of pesticide residues in food. *Food Control, 30*, 15–23.

Horikawa, T., Hayashi, J., & Muroyama, K. (2004). Controllability of pore characteristics of resorcinol–formaldehyde carbon aerogel. *Carbon, 42*, 1625–1633.

Ion, A. C., Ion, I., Culetu, A., Gherase, D., Moldovan, C. A., Iosub, R., et al. (2010). Acetylcholinesterase voltammetric biosensors based on carbon nanostructure-chitosan composite material for organophosphate pesticides. *Materials Science and Engineering C-Materials for Biological Applications, 30*, 817–821.

Jha, N., & Ramaprabhu, S. (2010). Development of Au nanoparticles dispersed carbon nanotube-based biosensor for the detection of paraoxon. *Nanoscale, 2*, 806–810.

Kandimalla, V. B., & Ju, H. X. (2006). Binding of acetylcholinesterase to multiwall carbon nanotube-cross-linked chitosan composite for flow-injection amperometric detection of an organophosphorous insecticide. *Chemistry, 12*, 1074–1080.

Kim, H.-J., Kim, W.-I., Park, T.-J., Park, H.-S., & Suh, D. J. (2008). Highly dispersed platinum–carbon aerogel catalyst for polymer electrolyte membrane fuel cells. *Carbon, 46*, 1393–1400.

Lee, J. H., Park, J. Y., Min, K., Cha, H. J., Choi, S. S., & Yoo, Y. J. (2010). A novel organophosphorus hydrolase-based biosensor using mesoporous carbons and carbon black for the detection of organophosphate nerve agents. *Biosensors and Bioelectronics, 25*, 1566–1570.

Li, Y. R., Gan, Z. Y., Li, Y. F., Liu, Q., Bao, J. C., Dai, Z. H., et al. (2010). Immobilization of acetylcholinesterase on one-dimensional gold nanoparticles for detection of organophosphorous insecticides. *Science China Chemistry, 53*, 820–825.

Li, Y. P., & Han, G. Y. (2012). Ionic liquid-functionalized graphene for fabricating an amperometric acetylcholinesterase biosensor. *Analyst, 137*, 3160–3165.

Liu, D. B., Chen, W. W., Wei, J. H., Li, X. B., Wang, Z., & Jiang, X. Y. (2012). A highly sensitive, dual-readout assay based on gold nanoparticles for organophosphorus and carbamate pesticides. *Analytical Chemistry, 84*, 4185–4191.

Machadoa, B. F., Morales-Torresa, S., Perez-Cadenas, A. F., Maldonado-Hodar, F. J., Carrasco-Marín, F., Silva, A. M. T., et al. (2012). Preparation of carbon aerogel supported platinum catalysts for the selective hydrogenation of cinnamaldehyde. *Applied Catalysis A: General, 425*, 161–169.

Maldonado-Hodar, F. J. (2012). Platinum supported on carbon aerogels as catalysts for the *n*-hexane aromatization. *Catalysis Communications, 17*, 89–94.

Marques, P. R., Nunes, G. S., dos Santos, T. C., Andreescu, S., & Marty, J.-L. (2004). Comparative investigation between acetylcholinesterase obtained from commercial sources and genetically modified drosophila melanogaster. Application in amperometric biosensors for methamidophos pesticide detection. *Biosensors and Bioelectronics, 20*, 825–832.

Norouzi, P., Pirali-Hamedani, M., Ganjali, M. R., & Faridbod, F. (2010). A novel acetylcholinesterase biosensor based on chitosan-gold nanoparticles film for determination of monocrotophos using FFT continuous cyclic voltammetry. *Journal of Electrochemistry Science, 5*, 1434–1446.

Rotariu, L., Zamfir, L.-G., & Bala, C. (2012). A rational design of the multiwalled carbon nanotube-7,7,8,8-tetracyanoquinodimethan sensor for sensitive detection of acetylcholinesterase inhibitors. *Analytica Chimica Acta, 748*, 81–88.

Sharma, S. P., Tomar, L. N. S., Acharya, J., Chaturvedi, A., Suryanarayan, M. V. S., & Jain, R. (2012). Acetylcholinesterase inhibition-based biosensor for amperometric detection of sarin using single-walled carbon nanotube-modified ferrule graphite electrode. *Sensors and Actuators B, 166*, 616–623.

Sing, K. S. W., Everett, D. H., Haul, R. A. W., Moscou, L., Pierotti, R. A., Rouquerol, J., et al. (1985). Reporting physisorption data for gas/solid systems with special reference to the determination of surface area and porosity. *Pure and Applied Chemistry, 57*, 603–619.

Stoytcheva, M., Zlatev, R., Velkova, Z., Valdez, B., Ovalle, M., & Petkov, L. (2009). Hybrid electrochemical biosensor for organophosphorus pesticides quantification. *Electrochimica Acta, 54*, 1721–1727.

Sun, X., Zhu, Y., & Wang, X. Y. (2012). Amperometric immunosensor based on deposited gold nanocrystals/4, 4-thiobisbenzenethiol for determination of carbofuran. *Food Control, 28*, 184–191.

Uutela, P., Reinila, R., Piepponen, P., Ketola, R. A., & Kostiainen, R. (2005). *Rapid Communications in Mass Spectrometry, 19*, 2950–2956.

Wang, K., Liu, Q., Dai, L. N., Yan, J. J., Ju, C., Qiu, B. J., et al. (2011). A highly sensitive and rapid organophosphate biosensor based on enhancement of CdS–decorated graphene nanocomposite. *Analytica Chimica Acta, 695*, 84–88.

Wei, M., Sun, L. G., Xie, Z. Y., Zhi, J. F., Fujishima, A., Einaga, Y., et al. (2008). Selective determination of dopamine on a boron-doped diamond electrode modified with gold nanoparticle/polyelectrolyte-coated polystyrene colloids. *Advanced Functional Material, 18*, 1414–1421.

Wei, S. L., Wu, D. C., Shang, X. L., & Fu, R. W. (2009). Studies on the structure and electrochemical performance of Pt/carbon aerogel catalyst for direct methanol fuel cells. *Energy Fuel, 23*, 908–911.

Wei, M., Xie, Z. Y., Sun, L. G., & Gu, Z. Z. (2009). Electrochemical properties of a boron-doped diamond electrode modified with gold/polyelectrolyte hollow spheres. *Electroanalysis, 21*, 138–143.

Wei, W., Zong, X. M., Wang, X., Yin, L. H., Pu, Y. P., & Liu, S. Q. (2012). A disposable amperometric immunosensor for chlorpyrifos-methyl based on immunogen/platinum doped silica sol–gel film modified screen-printed carbon electrode. *Food Chemistry, 135*, 888–892.

Wu, S., Zhang, L. L., Qi, L., Tao, S. Y., Lan, X. Q., Liu, Z. G., et al. (2011). Ultra-sensitive biosensor based on mesocellular silica foam for organophosphorous pesticide detection. *Biosensors and Bioelectronics, 26*, 2864–2869.

Zamfir, L.-G., Rotariu, L., & Bala, C. (2011). A novel, sensitive, reusable and low potential acetylcholinesterase biosensor for chlorpyrifos based on 1-butyl-3-methylimidazolium tetrafluoroborate/multiwalled carbon nanotubes gel. *Biosensors and Bioelectronics, 26*, 3692–3695.

Zejli, H., de Cisneros, J. L. H.-H., Naranjo-Rodriguez, I., Liu, B. H., Temsamani, K. R., & Marty, J.-L. (2008). Alumina sol–gel/sonogel-carbon electrode based on acetylcholinesterase for detection of organophosphorus pesticides. *Talanta, 77*, 217–221.

Zhang, L., Long, L. J., Zhang, W. Y., Du, D., & Lin, Y. H. (2012). Study of inhibition, reactivation and aging processes of pesticides using graphene nanosheets/gold nanoparticles-based acetylcholinesterase biosensor. *Electroanalysis, 24*, 1745–1750.

Zhang, L., Zhang, A. D., Du, D., & Lin, Y. H. (2012). Biosensor based on prussian blue nanocubes/reduced graphene oxide nanocomposite for detection of organophosphorus pesticides. *Nanoscale, 4*, 4674–4679.

Zhao, W., Ge, P. Y., Xu, J.-J., & Chen, H.-Y. (2009). Selective detection of hypertoxic organophosphates pesticides via PDMS composite based acetylcholinesterase-inhibition biosensor. *Environmental Science & Technology, 43*, 6724–6729.

Zhou, J., Zhuang, J. Y., Miró, M., Gao, Z. Q., Chen, G. N., & Tang, D. P. (2012). Carbon nanospheres-promoted electrochemical immunoassay coupled with hollow platinum nanolabels for sensitivity enhancement. *Biosensors and Bioelectronics, 35*, 394–400.